PassiveRETRO: Enabling Completely Passive Visible Light Localization for IoT Applications

***Abstract*—Identifying the accurate location of small objects is a key element of Internet of Things (IoT). This paper investigates the feasibility of tracking the real-time location of a completely passive retroreflector using visible light for IoT applications. Existing ultra-low power visible light retroreflector systems modulate light with a liquid crystal display (LCD) shutter, which is powered by a solar cell. However, the solar cell costs additional space exclusively for energy harvesting, and it may not be able to supply enough power to the advanced power-hungry LCD shutter and its driver circuit. To eliminate the power supply, we design, implement and evaluate PassiveRETRO, an enhanced retroreflector-based visible light localization system. The PassiveRETRO system** *completely eliminates the necessity of any electronic component* **on the IoT devices. Polarization-based modulation and bandpass optical filters are adopted to identify the retroreflected optical signal and create multiple channels. Each IoT device operates on a specific range of the visible light spectrum. Optical rotatory dispersion is further applied to mitigate the mutual interference among different channels. Experimental results from our prototyped system show that PassiveRETRO is robust to environmental reflection and can still achieve centimeter-level location accuracy when multiple IoT devices are deployed.**

***Index Terms*—Visible light localization, passive localization, Internet of Things, polarization, retroreflection.**

I. Introduction

As more "smart objects" continue to join the massive network of interconnected devices, called the Internet of Things (IoT), ubiquitous indoor localization has become a topic of interest for many applications [1]–[8]. Existing indoor localization approaches can be divided into two categories: client-based and server-based indoor localization. Client-based indoor localization [1]–[7], which is mainly suitable for navigation, is done directly on the device. Through receiving beacons from one or multiple anchors (i.e., access points), the device self-determines its position in global coordinates system. Server-based indoor localization [8], of which real-time locating system (RTLS) is a paradigm, uses multiple anchors to receive the beacons sent from the device and forward them to a local controller to compute the position of the device. Indoor RTLS, used to identify and localize devices in real-time, has many applications in asset tracking and indoor navigation, and can be of great importance in hospitals, airports, warehouses and schools. Typical applications include tracking medical devices in hospitals, locating robots in autonomous warehouses, and finding customers in a busy restaurant to serve food.

Visible light communication (VLC) as an ideal candidate for ubiquitous indoor localization uses light sources such as LED or fluorescent light and sensing hardware such as photodiodes and cameras to send and receive signals respectively through the modulation of light intensity at an imperceptible flickering frequency. Existing VLC localization systems use different features of optical signal, such as received signal strength (RSS), angle of arrival (AoA), polarization and light source patterns, to localize a device with respect to light sources of known coordinates [1]–[8]. These systems have demonstrated sub-meter localization accuracy and even great orientation accuracy. However, most of the VLC-based localization systems suffer from one downside, being the lack of a real-time backward channel from the device to the anchors, which leads to the necessity of expensive sensing hardware such as cameras [2]–[5], [7], or heavy computing at the device [1]–[7]. The RETRO system proposed in [8] sets up the real-time backward channel by using an LCD shutter to modulate the retroreflected light from a corner-cube retroreflector, which distinguishes the retroreflected optical signals from the environmental reflection and from the signals retroreflected from other IoT devices.

The retroreflector-based VLC system is first proposed and prototyped in RetroVLC [9], which exploits the nature of a retroreflector (i.e., reflecting the light back almost exactly along its incoming path). RetroVLC uses 3M Scotchlite retroreflective material and adopts on-off keying (OOK) modulation scheme for the uplink with an MCU-controlled LCD shutter. Pixelated VLC backscatter proposed in [10] extends the idea of RetroVLC by combining a plural of retroreflectors and LCD shutters to overcome the nonlinear responses of LCD state to voltage changes and generate multi-level signals. PassiveVLC [11] improves RetroVLC from the perspective of coding and modulation schemes. By replacing Manchester coding with Miller coding and designing a trend-based modulation and code-assisted demodulation scheme, PassiveVLC achieves 1 kbps uplink data rate which is 8x the data rate of RetroVLC. All the existing retroreflector-based VLC systems including [8] modulate the retroreflected light by an MCU-controlled LCD shutter, which requires a solar cell to supply power. For small IoT devices, the solar cell costs additional space exclusively for energy harvesting and may not be able to supply enough power to the power-hungry LCD shutter such as the advanced Pi-cell [12] and its driver circuit under normal indoor illumination. Therefore, we seek to completely eliminate the electronic components on the IoT device and render it truly passive.

In this paper, we propose and prototype the PassiveRETRO system - an enhanced retroreflector-based visible light localization system, which retains the advantages of the RETRO system [8], such as being implementable on any single unmodified light source, having immediate feedback from the retroreflector to the anchors, and being capable of localizing IoT devices with ultra-low power and no computational capability at the devices. It also improves the RETRO system by rendering the RETRO tag completely passive. A general LCD shutter consists of two linear polarizers and one liquid crystal layer in between. PassiveRETRO system splits the general LCD shutter into two parts; one linear polarizer is attached

to the RETRO tag while the other linear polarizer plus the liquid crystal layer are mounted on the light source. Since the liquid crystal layer is mounted on the light source, the power-hungry issue of RETRO system [8], which restricts the type of the LCD shutter, is inherently resolved. This advantage allows the liquid crystal layer with high power and low response time, such as that of the advanced Pi-cell [12], to be adopted as a fast speed modulator, which mitigates the baseband background interference (e.g., 60 Hz background light) to the retroreflected optical signals. Bandpass optical filters are attached to both the RETRO tag and the photodiode (PD) mounted on the light source to identify different RETRO tags. Each tag operates on a specific range of the visible light spectrum. Optical rotatory dispersion [3] is further leveraged to alleviate the mutual interference among different channels. In Section II, we briefly describe the concept of the original RETRO system [8] and introduce the concepts of polarization-based modulation, optical rotatory dispersion, and the idea of PassiveRETRO system. In Section III, we highlight the system design challenges and their corresponding solutions. Advanced design for improving the system performance is presented in Section IV. Section V demonstrates the prototyped system and the evaluation results. Section VI concludes the paper.

In summary, we make the following three key contributions:

- We design and implement an enhanced retroreflector-based visible light localization system, called PassiveRETRO, which retains all the advantages of the RETRO system [8] and improves it by rendering the RETRO tag completely passive. The enhancement circumvents the necessity of a solar cell, which saves at least 33% of the space of the RETRO tag [9], [11], and enables the utilization of high-power and low-response-time liquid crystal layer (e.g., that of Pi-cell), which inherently mitigates the baseband background interference.
- We propose advanced designs for the basic PassiveRETRO system, such as adding an optical rotatory dispersor to reduce the mutual interference among different channels, customizing the thickness of the dispersor to maximize the signal-to-interference-plus-noise ratio (SINR) for each channel, and devising the bandwidth of each bandpass optical filter to guarantee the fairness of different channels in terms of SINR.
- We evaluate the impacts of advanced designs and the system performance of PassiveRETRO in terms of location accuracy and mutual interference level with single and multiple devices by numerical analysis and extensive experiments. When multiple devices are deployed, we observe centimeter-level location accuracy.

II. Overview

In this section, we first briefly review the system diagram of RETRO [8], and then introduce the basics of polarization-based modulation, including how to generate and detect polarized light and how to modulate the polarization. We also introduce the way that the optical rotatory dispersor varies the polarization and the basic setup of PassiveRETRO system.

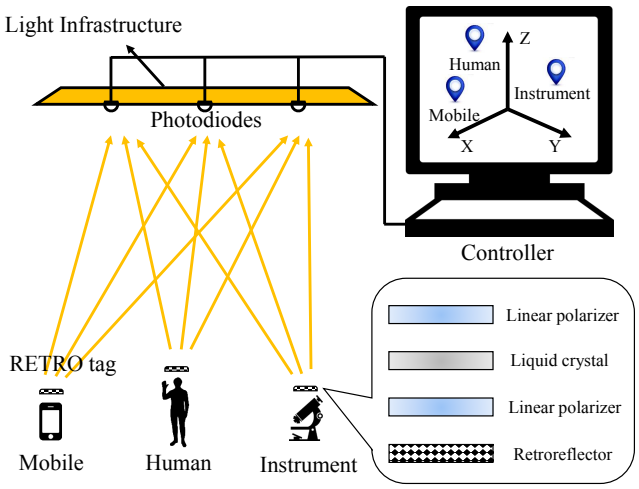

Fig. 1: The architecture of RETRO system

A. RETRO system

In the RETRO system [8] (Figure 1), a RETRO tag is attached to each tracking object, such as mobile device, wearable device or even passive instrument. The RETRO tag is composed of an LCD shutter, which consumes tens of μW with its driver circuit, and a retroreflector, from which the retroreflected light is modulated by the LCD shutter for distinguishing environmental reflection and different IoT devices. The retroreflected optical signal strength is measured by multiple photodiodes (i.e., landmarks) mounted on a single unmodified light source. As the retroreflector changes its location and orientation, the RSS of each PD varies correspondingly. A Lambertian light source retroreflection path loss model is derived to characterize the relationship between the location and orientation of the retroreflector and the RSS of each PD. The RSS of each PD is input to a received signal strength indicator (RSSI) and trilateration localization algorithm to estimate the location and orientation of the IoT device.

B. Polarization-based modulation

One of the basic properties of light signals is polarization, or the direction of oscillation of a beam's electric field. White light emitted by most common light sources, like fluorescent light, incandescent light, or LEDs, is unpolarized, meaning each beam consists of light with mixed polarization. The device transforming unpolarized light into polarized light is called polarizer, which is commonly used in many applications - LCD screens, sunglasses, camera filters, etc. Linear polarizers are the polarizers that selectively block the incident light based on Malus's law. Given the intensity of the incident light as I_0 and the polarizing angle between the incident light and the linear polarizer as θ, Malus's law states that the intensity of the polarized light after passing through the linear polarizer is $I_\theta = I_0 \cos^2 \theta$. Therefore, according to Malus's law, if $\theta = 0$, the incident light will completely pass through, while if $\theta = 90°$, the incident light will be completely blocked.

The polarization of light can be modulated using a liquid crystal layer as a modulator. Taking the Twisted Nematic (TN)

liquid crystal as an example, when a voltage is not applied, the general commodity TN liquid crystal layer acts like a polarization rotator, which takes linearly polarized light and rotates the direction of its polarization by 90°. However, when a voltage is applied, the molecules of the liquid crystal layer realign and no longer rotate the polarization of the incident light. Therefore, if we use another linear polarizer that has a polarization that is orthogonal to that of the incident light before passing through the liquid crystal layer, the incident light will be blocked if a high voltage is applied and the incident light will pass through without attenuation if no voltage is applied. Accordingly, the intensity of the light that passes through the two linear polarizers and the liquid crystal layer corresponds to the voltage applied to the liquid crystal layer and we can adjust the applied voltage to perform modulation by switching between the opaque and transparent states.

C. Optical rotatory dispersion

To identify and localize different IoT devices simultaneously, bandpass optical filters are adopted to separate different channels. By placing the bandpass optical filters on both the RETRO tags and the PDs installed on the light source, location dependent RSS can be measured individually for each channel, which uses a small range of the visible light spectrum. Bandpass optical filters alone, however, are not good enough for isolating channels, since general commodity filters only weaken certain wavelengths outside the desirable range, rather than completely blocking them out. These wavelengths interfere with other channels and result in less accurate localization for the adjacent channels. To mitigate the inter-channel interference, we employ a technique called optical rotatory dispersion (ORD) [3] to tune the polarization for different wavelengths. ORD is a property of some materials that rotate the polarization of light to different extents depending on the wavelength of light. After the light passes through the optical rotatory dispersor, shorter wavelengths are rotated more than longer wavelengths, per unit distance. ORD has been studied for decades and is widely employed in chemistry, pharmaceutics, and mineralogy for quantitative study, determination of absolute configuration, conformational study and equilibrium study. Denoting the thickness of a dispersor by L and the function of wavelength λ which describes the rotation of light polarization per unit distance by $n(\lambda)$, the polarization of a beam with wavelength λ is rotated by $\psi(\lambda) = n(\lambda)L$. The mechanism we employ so that optical rotatory dispersion mitigates the mutual interference among different channels will be demonstrated in detail in Section IV-A.

D. PassiveRETRO system

Now we describe the design of the PassiveRETRO system. As shown in Figure 2, the PassiveRETRO system basically consists of two parts - the VLC transceiver part which is shown in the top bubble and the PassiveRETRO tag part which is shown in the bottom bubble. Inspired by the designs in [3] and [13], the PassiveRETRO system splits the LCD shutter into two parts; one linear polarizer and one liquid

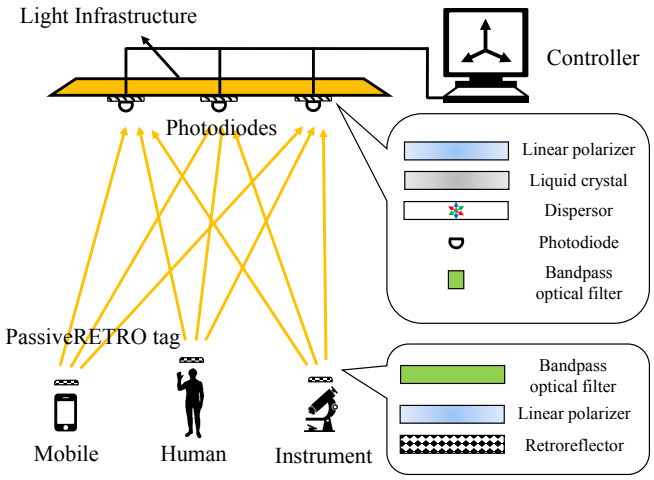

Fig. 2: PassiveRETRO system diagram

crystal layer are installed on the light source for polarization-based modulation, and another linear polarizer is placed on top of the retroreflector to modulate the retroreflected light. In both [3] and [13], a dispersor is mounted on the liquid crystal layer for the purpose of communication. In [3], to tackle the arbitrary orientation problem of mobile devices, optical rotatory dispersion is adopted to change the Binary Intensity Shifting Keying (BISK) of normal LCD shutters to Binary Color Shift Keying (BCSK), which minimizes the impact of the orientation variation of mobile devices on the RSS. In [13], optical rotatory dispersion is applied to separate the RGB channels and enable a point-to-point (PTP) communication system that is analogous to a 3x3 multi-input multi-output (MIMO) system. However, the dispersor used in the PassiveRETRO system is for a completely different goal than those in [3] and [13]. In Figure 2, the green channel is provided as an example. If we replace the green bandpass optical filter on the retroreflector by a red bandpass optical filter, the retroreflected signals will be significantly, but not one hundred percent, filtered out by the green bandpass optical filter mounted on the PD. Therefore, optical rotatory dispersion is leveraged to alleviate the mutual interference among different channels. Since only the bandpass optical filter and the linear polarizer are deployed on the retroreflector, the PassiveRETRO tag is operating with no electronic component so that it does not require any power supply unit.

Note that although the polarization of light cannot be perceived by human eyes as stated in [3] and [13], very low modulation rate still creates flickering problem due to the change of polarization by reflection [14]. The reflected light from the surfaces of any object is linearly polarized when the incidence angle is above a certain value (i.e., Brewster's angle [14]) with its electric field vectors perpendicular to the plane of incidence and parallel to the plane of the surface from which it is reflected. Therefore, if the polarization of the linearly polarized light is modulated by the liquid crystal layer at a relatively low speed (e.g., less than 30 Hz), the flickering problem is considerable. The PassiveRETRO system allows

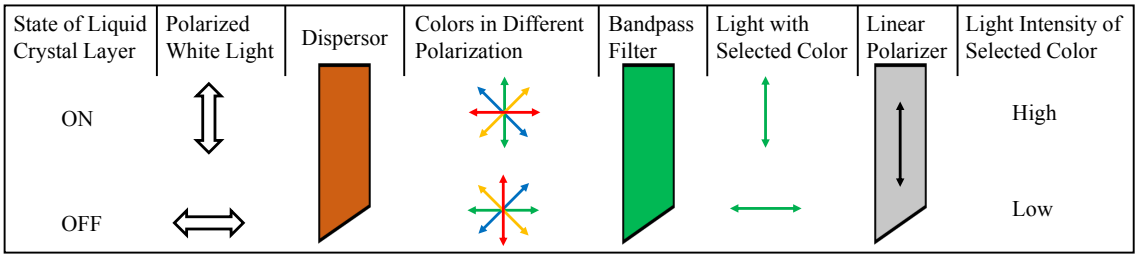

Fig. 3: When the state of liquid crystal layer is changed between ON and OFF, the received light intensity of the selected color is varying between high and low.

the liquid crystal layer to modulate at the fastest speed, which inherently circumvents the flickering issue.

Also note that since the effective reflecting area [8], from which the emitted light rays are retroreflected back to the PD, depends on the size of the front face of a single corner-cube retroreflector, the linear polarizer, the liquid crystal layer and the dispersor do not have to cover the whole surface of the light source. Although the PassiveRETRO system can be implemented on any unmodified light infrastructure, the ideal structure of the light source would have the linear polarizer, the liquid crystal layer and the dispersor only covering the surrounding area of the PD. The light emitted around the PD would be the brightest, while the light emitted from other places on the light source surface would be as dark as possible for the purpose of maximizing the performance of the localization system while introducing no glaring issue.

III. PassiveRETRO Basic Design

In this section, we highlight the challenges of designing a completely passive visible light retroreflector based localization system and demonstrate the corresponding solutions that are adopted in the PassiveRETRO system design.

A. Environmental Reflection

Light reflected by walls, floors, ceilings and other objects acts as an interferer to the retroreflected light from the IoT devices if we directly measure the intensity of the retroreflected light for the purpose of localization. To handle the environmental reflection problem, the general approach is to have a reader. The reader broadcasts the interrogating signal and senses the strength of the reflected signal from the tracking object at a certain frequency. The measured RSS carries the information of the unique identity and the distance between the reader and the tracking object. The paradigms that utilize this approach are RFID, bar-code and QR-code, etc. In [8], to distinguish the retroreflected optical signal from environmental reflection, an LCD shutter is attached to the retroreflector to modulate the retroreflected optical signal. By transitioning between transparent and opaque states, LCD shutter can approximate a square wave signal at a certain modulation frequency. The amplitude of the square wave signal is computed by Fast Fourier Transform (FFT) processing of the time domain data samples. As the modulation frequency increases, the amplitude of the square wave signal deteriorates. This is because of the response time of the liquid crystal layer. A general TN liquid crystal layer [15] takes 5 ms to transit from untwisted state to twisted state and 2 ms to transit back from twisted state to untwisted state. Faster LCD shutters, like Pi-cell [15], lower both the rise and the fall response time to less than 1 ms. However, Pi-cell costs much more power than TN shutter, which limits the applicable scenarios of Pi-cell.

In the PassiveRETRO system, one linear polarizer and the liquid crystal layer are deployed on the light source, which makes the light source an interrogator. Another linear polarizer is attached to the front face of the retroreflector to distinguish the retroreflected optical signals from the environmental reflection and among different IoT devices. As shown in Figure 3, if the linear polarizer on the retroreflector is perfectly aligned with the linear polarizer on the light source, the intensity of the retroreflected light switches between high and low when the state of the liquid crystal layer switches between ON and OFF. Note that the environmental reflection indeed affects the polarization of the incident light [14], which means that if a linearly polarized light beam incident on a reflecting surface with the incidence angle larger than zero, the intensity of the reflected light beam will be lower if the polarization of the incident light beam is not parallel to the reflecting surface and vice versa. Therefore, the environmental reflection generates reflected optical signals at the same modulated frequency as that of the retroreflected optical signal. Nevertheless, only the surrounding area of the PD emits the polarized light, which means that the incidence angle of the polarized light beam to any surface of objects will be zero if the corresponding reflected polarized light beam reaches back to the PD. To handle the environmental reflection interference generated from one light source to another, different modulation frequencies can be used for adjacent light sources. The polarization-based modulation solution is capable of distinguishing the retroreflected optical signals from the environmental reflection. However, the solution cannot distinguish the retroreflected optical signals from different IoT devices.

B. Distinguishing Different Devices

In order to simultaneously localize different IoT devices with acceptable interference among them, bandpass optical filters are adopted to assign different channels for different IoT devices. One bandpass optical filter is customized to the same size of the front face of retroreflector and used to fully cover the retroreflector. The other bandpass optical filter is customized to the same size of the active sensing

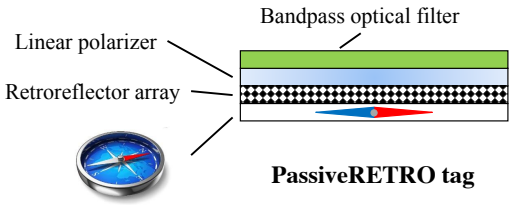

Fig. 4: Structure of PassiveRETRO tag

area of a PD and used to fully cover the PD. The bandpass optical filters can be manufactured as lightweight thin films, of which the thickness is only 2 mm [16]. Since multiple channels are to be sensed by one of the sensing units on the light source at the same time, the sensing unit can be manufactured as a PD array, which is similar to the structure of the sensing unit of the color sensor TCS230 [17]. As shown in Figure 3, the bandpass optical filters on the retroreflector and the PD selectively pick the polarized white light within a specific wavelength range and isolate the corresponding channel. However, general bandpass optical filters do not perfectly filter out the light outside the desired wavelength range, which results in considerable interference to adjacent channels, especially when the required number of channels is large. To alleviate the inter-channel interference issue, optical rotatory dispersion is adopted and the mechanism will be demonstrated in details in Section IV-A.

C. Arbitrary Orientation of Devices

The rotation of IoT devices changes the polarizing angle between the linear polarizer on the light source and the linear polarizer on the retroreflector, which will affect the intensity difference of the two states shown in Figure 3. Referring to the right sub-figure of Figure 5 in [3], the intensity difference fluctuates significantly when the receiver changes its orientation. The arbitrary orientation issue has been considered both in [3] and [18]. In [3], an optical rotatory dispersor is mounted on the light source to rotate the polarization of incident light based on wavelength and the receiver measures the color difference in RGB domain instead of light intensity difference. In [18], the polarization of the liquid crystal layer on the light source is electronically tuned in discrete time slots to search for a proper polarization angle that gives a high intensity contrast. In PassiveRETRO system, we propose a new way to tackle the arbitrary orientation problem. As shown in Figure 4, at the bottom of the PassiveRETRO tag, a lightweight compass is attached to align the linear polarizer using Earth's magnetic field. The polarization of the linear polarizer on the light source is fixed. Different IoT devices using different channels have their corresponding optimal polarization angles that give the highest intensity contrast. The optimal polarization angles can be fixed by the compass needle even if the IoT devices vary in orientation.

D. Localization Algorithm

Each IoT device utilizes a specific range of the visible light spectrum. After measuring the strength of the retroreflected optical signal from one IoT device by n ($n \geq 5$) sensing units mounted on the light source, we substitute the measured RSSs to the left side of (10) in [8], which characterizes the relationship between the location and orientation of the retroreflector and the RSS of each PD. The RSSI and trilateration based localization is framed as an optimization process minimizing the square errors between the left and the right sides of (10) in [8]. The Levenberg-Marquardt algorithm is adopted to resolve the optimization problem and estimate the 2D/3D location of the IoT device. In [8], P_t in (10), which denotes the transmitted optical power multiplied by the retroreflection loss, is estimated by fitting the experimental results to the theoretical results. For the PassiveRETRO system, the value of P_t needs to be estimated once for each channel since different channels have different path losses caused by bandpass optical filters.

IV. PassiveRETRO Advanced Designs

In this section, we present the advanced designs of PassiveRETRO system to improve the localization performance, such as adding an optical rotatory dispersor to reduce the inter-channel interference, optimizing the thickness of dispersor to enhance the SINR for each channel, and adjusting the bandwidth of each bandpass optical filter for the consideration of fairness in terms of the SINR of each channel.

A. Add an optical rotatory dispersor

As discussed in Section III-B, due to the imperfection of bandpass optical filters, optical rotatory dispersion is adopted to mitigate the inter-channel interference. We compare the system without and with a dispersor in Figure 5 and Figure 6, respectively. As shown in Figure 5, the linear polarizer on the retroreflector is parallel or orthogonal to the linear polarizer on the light source. After the polarized white light passes through the green bandpass optical filter, some blue and yellow light with the same polarization as that of the green light is retained. As the liquid crystal layer switches between ON and OFF, the intensity contrast of blue and yellow light is relatively large since the polarization is either parallel or orthogonal to the linear polarizer on the retroreflector. As shown in Figure 6, the linear polarizer on the retroreflector is parallel or orthogonal to the polarization direction of the target wavelength (i.e., green). After the polarized white light passes through the optical rotatory dispersor, the polarization of the blue and yellow light is rotated by certain angles which depend on the material and the thickness of the dispersor. The intensity contrast of blue and yellow light is thereby reduced since the difference of polarizing angle between the polarization of the blue and yellow light and the linear polarizer on the retroreflector is decreased as the liquid crystal layer switches states. The capability of optical rotatory dispersion to mitigate the inter-channel interference is validated by experiments in Section V.

B. Thickness of Dispersor

Recall that after passing through an optical rotatory dispersor, the polarization of a beam with wavelength λ is rotated by $\psi(\lambda) = n(\lambda)L$, where L is the thickness of the dispersor

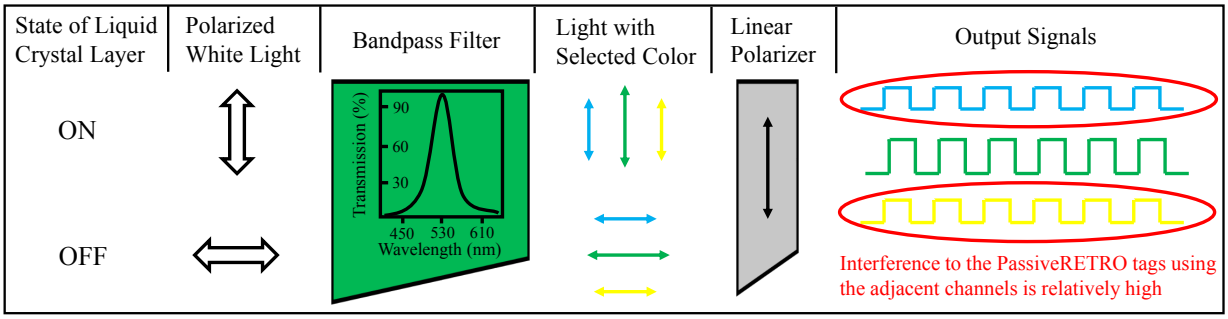

Fig. 5: Without adding the optical rotatory dispersor, the interference produced by each channel to the adjacent channels is relatively strong due to the imperfection of bandpass optical filter.

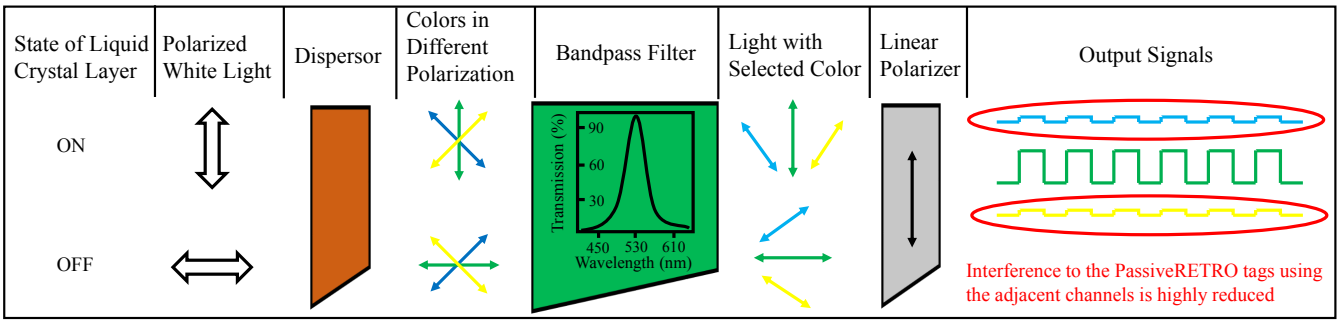

Fig. 6: After adding the optical rotatory dispersor, the polarization of yellow light and blue light are rotated such that the difference of polarizing angle between the yellow and blue light and the linear polarizer is reduced when the state of liquid crystal layer switches between ON and OFF. Therefore, the interference produced by the green channel to the yellow and the blue channels is mitigated.

and $n(\lambda)$ is a function of wavelength λ which describes the rotation of light polarization in unit distance. For a given type of dispersor material, the thickness of the dispersor affects both the RSS for the target channel and the interference level caused by the target channel to the adjacent channels.

After passing through the bandpass optical filter, the intensity of a light beam with wavelength λ is $I_b(\lambda) = I_0(\lambda)r(\lambda)$, where $I_0(\lambda)$ is the intensity of the light beam with wavelength λ before passing through the bandpass optical filter and $r(\lambda)$ is the transmittance factor of the bandpass optical filter for wavelength λ.

After passing through the linear polarizer, based on Malus's law, the intensity of a light beam with wavelength λ is

$$I_p(\lambda, \theta, L) = I_b(\lambda) cos^2(\psi(\lambda) - \theta),$$

where θ is the polarizing angle between the linear polarizer on the light source and the linear polarizer on the retroreflector.

Considering the two states of liquid crystal layer, between which the polarizing angle is rotated by 90°, the RSS for a target channel is

$$S = |\int_{380}^{750} I_p(\lambda, \theta, L)d\lambda - \int_{380}^{750} I_p(\lambda, \theta + 90°, L)d\lambda|.$$

In order to maximize the RSS for a target channel, the thickness L can be chosen by resolving the optimization problem $\arg\max_L S$. Without considering inter-channel interference, the solution of $\arg\max_L S$ is $L = 0$. This is because without optical rotatory dispersion, all the wavelengths with $r(\lambda) > 0$ will have the maximum intensity contrast. However, if $L = 0$, the interference caused by the target channel to the adjacent channels is considerable, especially when the number of required channels is large and the central wavelength of channels are close to each other.

The interference caused by the target channel to another channel can be quantified as

$$I = |\int_{380}^{750} I_p(\lambda, \theta, L) r_a(\lambda) d\lambda - \int_{380}^{750} I_p(\lambda, \theta + 90°, L) r_a(\lambda) d\lambda|,$$

where $r_a(\lambda)$ is the transmittance factor of the bandpass optical filter using the channel that is interfered by the target channel. Denote the SINR of channel j by $SINR_j$, the thickness L can be determined by solving the optimization problem

$$\arg\max_L \sum_j SINR_j$$
$$s.t.\ SINR_j > T, \forall j,$$

where T is the minimum threshold of SINR that is required to achieve the acceptable localization performance.

Now we use some numerical results to evaluate the impact of the thickness of dispersor on the SINRs of different channels. Assume we have three channels, of which the central wavelengths (CW) are at 610 nm, 545 nm and 480 nm.

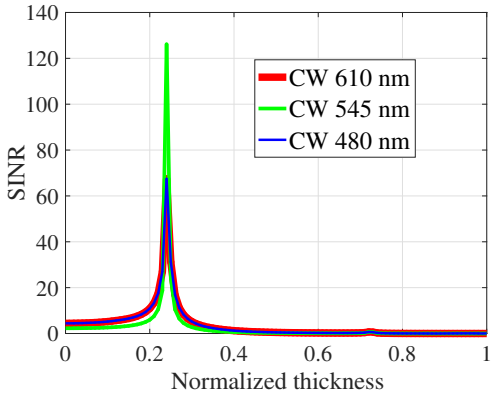

Fig. 7: As the thickness of dispersor increases, the variation of SINRs for different channels shows that the customization of the optimal thickness of dispersor is capable of significantly improving the SINRs.

The transmission characteristics curves of the three bandpass optical filters follow a distribution that is very close to the probability density function (PDF) of a Gaussian random variable [17]. The light spectrum is evenly distributed across the visible light range [3] and the function $n(\lambda)$ is linear [19]. The numerical results are shown in Figure 7. The best thickness of the dispersor is the same for all the three channels. According to the numerical results, the customization of the optimal thickness of the dispersor is capable of significantly improving the SINRs by over 10 times. In Section V, we use the commercial off-the-shelf (COTS) dispersor. In our future work, we will experimentally evaluate the impact of customizing the thickness of the dispersor on the SINRs of different channels.

C. Bandwidth of bandpass optical filter

To allow more IoT devices to be localized simultaneously, narrower bandwidth has to be assigned to each channel to provide more channels, which will result in lower RSS for each channel. The bandwidth allocation of each bandpass optical filter should depend on the light spectrum of the light source. If the intensity of light spectrum for a target channel is low, the allocated bandwidth for the target channel should be wide in order to improve the RSS and also the allocated bandwidth for the adjacent channels should be narrow for the purpose of mitigating the interference to the target channel. In Section V, we show by experiments the impact of altering the bandwidth of bandpass optical filter on the SINR of different channels.

V. Experiments

In this section, extensive experiments are conducted to i) validate the capability of optical rotatory dispersion on mitigating the inter-channel interference and improving the SINR for each channel; ii) evaluate the impact of changing the bandwidth of bandpass optical filter on the SINR of each channel; iii) evaluate the localization performance when a single IoT device exists; iv) evaluate the localization performance when multiple IoT devices coexist.

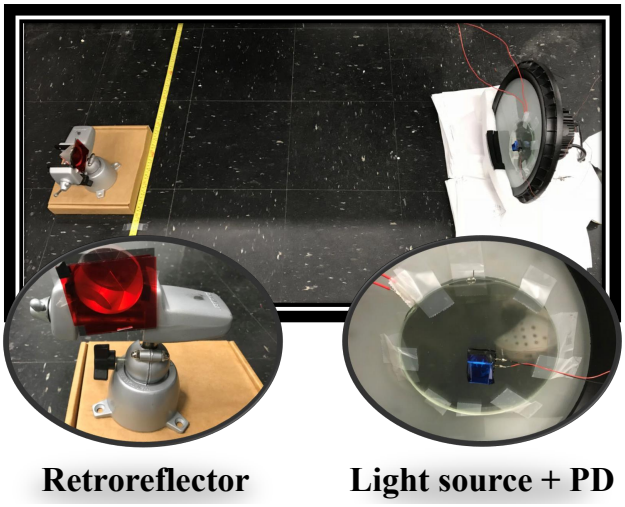

Fig. 8: Testbed of the PassiveRETRO system

A. Testbed settings

As shown in Figure 8, in the prototyped PassiveRETRO system, we utilize COTS LED light source provided by Solid Apollo [20]. Two linear polarizing films from Amazon [21] are used - one mounted on the light source to turn the unpolarized white light into polarized white light, one mounted on the retroreflector to selectively attenuate the incident light beam. The polarizing angle between two linear polarizers is set to 90° for the experiments without dispersor and set to different wavelength dependent angles for the experiments with dispersor. We use the same circular corner-cube retroreflector PS976 [22] as that used in [8]. The transparent color correction lighting gel filters from Amazon [23] are adopted as the bandpass optical filters, among which the red, green and blue filters are selected to form three separated channels. Two circular LCDs from Liquid Crystal Technologies [15] are used for the liquid crystal layer and the dispersor, respectively. The LCD used as liquid crystal layer is rotated by 45°, which will eliminate the ORD effect when the polarized light passes through it. This is due to a ployimide (PI) alignment layer [24] rubbed on the liquid crystal. The PD S6968 is provided by Hamamatsu Photonics [25] and its sensing area is 150 mm^2. The PD works in photoconductive mode to measure the light intensity. As shown in Fig. 9, the PD is driven by a 10 V DC and cascaded with a 6.8kΩ resistor. The received optical power is linearly proportional to the output voltage of the resistor. We connect light intensity measurement circuit to an oscilloscope (Tektronix MDO4034-3) and set the sampling rate to 1 MS/s. The recorded data is processed in MATLAB through Fast Fourier Transform (FFT) to compute the signal amplitude. Denoting the FFT length by N, the amplitude of the 1st harmonics in frequency domain by A_f, and the

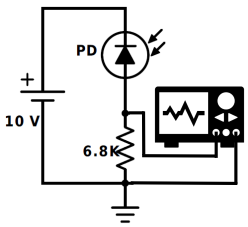

Fig. 9: Light intensity measurement circuit

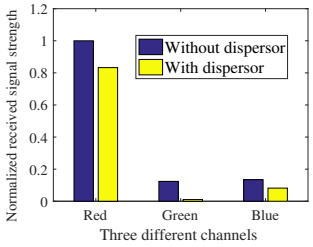

Fig. 10: RSS of red channel with and without dispersor

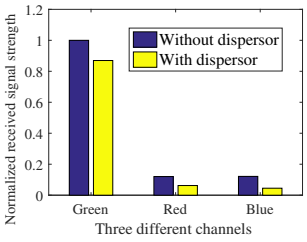

Fig. 11: RSS of green channel with and without dispersor

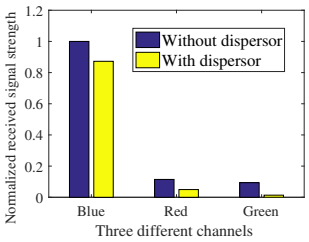

Fig. 12: RSS of blue channel with and without dispersor

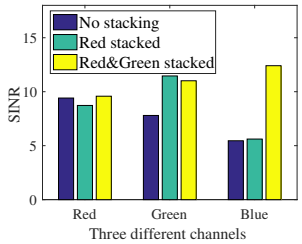

Fig. 13: Varying the bandwidth of channels

amplitude of the square wave in time domain by A_t, we have $A_f = A_t/(N/2)$. The localization algorithm is the same as that used in [8]. The vertical distance between the light source and the retroreflector is set to 1 meter.

B. Experiment Results

To evaluate the capability of optical rotatory dispersion to mitigate the inter-channel interference, we conduct two sets of experiments - one with a dispersor mounted on the light source and one without it. For each set of experiments, we place a red, green, or blue bandpass optical filter on the PD and measure the RSS for three cases: i) red filter; ii) green filter; iii) blue filter mounted on the retroreflector. As shown in Figure 10, adding an optical rotatory dispersor slightly decreases the RSS for the red channel. This is because the dispersor rotates the polarization of the wavelengths within the desired range of the red bandpass optical filter, which results in less intensity contrast. Nevertheless, the interference caused by the green and blue channels to the red channel is reduced significantly, especially the interference from the green channel. The same analysis applies to Figures 11 and 12. As a result of adding the optical rotatory dispersor, the SINRs of red, green and blue channels are improved by 231%, 283% and 288%, respectively. Note that since we use the COTS liquid crystal layer to serve as the optical rotatory dispersor, the thickness of the dispersor is not optimized. By customizing the dispersor carefully with the bandwidth and the light source spectrum taken into account, the SINR improvement is expected to be much more remarkable.

To evaluate the impact of altering the bandwidth of different bandpass optical filters on the SINRs of different channels, we use a filter stacking method to emulate the narrowing process of bandwidth. For the three cases, which are no stacking, red stacked, and red&green stacked, the SINRs of red, green and blue channels are shown in Figure 13. For the case of no stacking, we only place one piece of filter [23] on the retroreflector for each channel. For the case of red stacked, we add one more piece of red filter on the retroreflector when we measure the RSS for the red channel and the interference caused by the red channel to the green and blue channels. For the case of red&green stacked, we add one more piece of red filter and one more piece of green filter on the retroreflector when we measure the RSS for the red and green channels and the interference caused by the red and green channels to the other channels. Without stacking, the SINR of the red channel is the strongest. Therefore, based on the bandwidth adjustment idea elaborated in Section IV-C, the bandwidth of the red channel should be narrower in order to mitigate its interference to the green and blue channels. With red stacked, both the SINRs of the green and blue channels improve, especially the SINR of the green channel. With red&green stacked, both the SINRs of the red and blue channels improve, especially the SINR of the blue channel. As a consequence, the SINRs of all the three channels have been improved by the bandwidth adjustment, which validates the idea proposed in Section IV-C.

For the evaluation of localization performance, we adopt the same settings used in [8]. We input the measured RSSs to the RSSI and trilateration based localization algorithm to evaluate the 2D location accuracy on the horizontal plane where the vertical distance between the light source and the retroreflector is 1 meter, and the 3D location accuracy where the vertical distance between the light source and the retroreflector is unknown. In Figures 14 and 15, we measure the location accuracy for each channel when only one device is deployed. When the vertical distance is known, for the red channel, the location errors are less than 2 cm in 90% of the cases and the median error is 1 cm; for the green and blue channels, the location errors are less than 3.5 cm in 90% of the cases and the median error is 2 cm. When the vertical distance is unknown, for the red channel, the location errors are less than 4 cm in 90% of the cases and the median error is 1.5 cm; for the green channel, the location errors are less than 10 cm in 90% of the cases and the median error is 5 cm; for the blue channel, the location errors are less than 14 cm in 90% of the cases and the median error is 7 cm. The localization performance is comparable to that of the RETRO system [8]. The location errors of the green and blue channels are higher than those of the red channel. This is because the green and blue light emitted from the light source have less intensity than that of the red light.

In Figures 16 and 17, we measure the location accuracy for each channel when the red, green and blue devices are all deployed. When we measure the RSS for one channel, the other two interfering devices are placed at the projection of the PD on the horizontal plane. When the vertical distance is known, for the red channel, the location errors are less than 3 cm in 90% of the cases and the median error is 2 cm; for the green channel, the location errors are less than 4.5 cm in 90% of the cases and the median error is 3 cm; for the blue

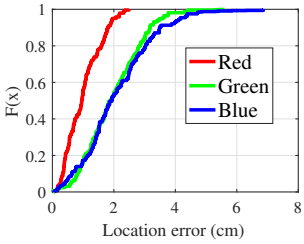

Fig. 14: CDF of 2D location error for a single device

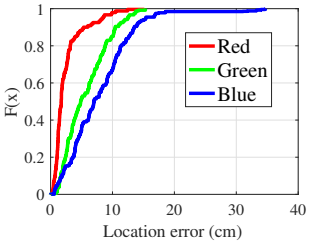

Fig. 15: CDF of 3D location error for a single device

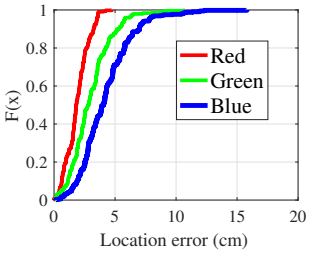

Fig. 16: CDF of 2D location error for multiple devices

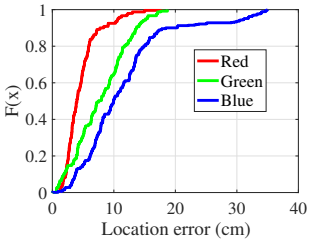

Fig. 17: CDF of 3D location error for multiple devices

channel, the location errors are less than 6.5 cm in 90% of the cases and the median error is 4 cm. When the vertical distance is unknown, for the red channel, the location errors are less than 7.5 cm in 90% of the cases and the median error is 4 cm; for the green channel, the location errors are less than 12 cm in 90% of the cases and the median error is 7.5 cm; for the blue channel, the location errors are less than 16 cm in 90% of the cases and the median error is 10 cm. The location errors when multiple devices are deployed are slightly increased when compared to the case where only a single device is deployed at each time. However, the localization performance is still remarkable when compared to that of other existing visible light localization systems [1]–[8]. Since we use the COTS hardware in the experiments, the localization performance is not optimized. In our future work, we will experimentally customize the bandwidth of bandpass optical filters, the thickness of the dispersor, the positions of LEDs and the light spectrum of the light source. The customization is expected to further enhance the localization performance including but not limited to the range of the localization system, the location accuracy, and the number of IoT devices.

VI. Conclusion

In this paper, we propose and prototype an enhanced retroreflector-based visible light localization system PassiveRETRO. Embracing all the advantages of the RETRO system [8], such as the utilization of any single unmodified light source, providing a real-time feedback channel from the retroreflector to the landmarks, eliminating the requirements of computational capability at the devices, PassiveRETRO further improves RETRO system by rendering the RETRO tag completely passive. The improvement saves the RETRO tag's space occupied by solar cell and enables the utilization of high-power and low-response-time liquid crystal layer such as that of the advanced Pi-cell [12]. Extensive experimental results demonstrate that PassiveRETRO achieves remarkably good performance, and centimeter-level location error when multiple IoT devices are deployed.

References

[1] L. Li, P. Hu, C. Peng, G. Shen, and F. Zhao, "Epsilon: A Visible Light Based Positioning System," in *USENIX NSDI*, 2014, pp. 331–343.

[2] Y.-S. Kuo, P. Pannuto, K.-J. Hsiao, and P. Dutta, "Luxapose: Indoor positioning with mobile phones and visible light," in *ACM MobiCom*, 2014, pp. 447–458.

[3] Z. Yang, Z. Wang, J. Zhang, C. Huang, and Q. Zhang, "Wearables can afford: Light-weight indoor positioning with visible light," in *ACM MobiSys*, 2015, pp. 317–330.

[4] C. Zhang and X. Zhang, "LiTell: Robust indoor localization using unmodified light fixtures," in *ACM MobiCom*, 2016, pp. 230–242.

[5] Z. Zhao, J. Wang, X. Zhao, C. Peng, Q. Guo, and B. Wu, "NaviLight: Indoor Localization and Navigation Under Arbitrary Lights," in *IEEE INFOCOM*, 2017.

[6] C. Zhang and X. Zhang, "Pulsar: Towards ubiquitous visible light localization," in *ACM MobiCom*, 2017, pp. 208–221.

[7] S. Zhu and X. Zhang, "Enabling high-precision visible light localization in today's buildings," in *ACM MobiSys*, 2017, pp. 96–108.

[8] S. Shao, A. Khreishah, and I. Khalil, "RETRO: Retroreflector based visible light indoor localization for real-time tracking of IoT devices," in *IEEE INFOCOM*, 2018.

[9] J. Li, A. Liu, G. Shen, L. Li, C. Sun, and F. Zhao, "Retro-VLC: Enabling battery-free duplex visible light communication for mobile and iot applications," in *ACM HotMobile*, 2015, pp. 21–26.

[10] S. Shao, A. Khreishah, and H. Elgala, "Pixelated VLC-backscattering for self-charging indoor IoT devices," *IEEE Photonics Technology Letters*, vol. 29, no. 2, pp. 177–180, 2017.

[11] X. Xu, Y. Shen, J. Yang, C. Xu, G. Shen, G. Chen, and Y. Ni, "Passivevlc: Enabling practical visible light backscatter communication for battery-free iot applications," in *ACM MobiCom*, 2017, pp. 180–192.

[12] Liquid Crystal Technologies, http://www.liquidcrystaltechnologies.com/tech_support/Pi_Cell.htm, [Online; accessed 4-May-2017].

[13] C.-L. Chan, H.-M. Tsai, and K. C.-J. Lin, "Poli: Long-range visible light communications using polarized light intensity modulation," in *ACM MobiSys*, 2017, pp. 109–120.

[14] Georgia State University, http://hyperphysics.phy-astr.gsu.edu/hbase/hph.html, [Online; accessed 1-Jan-2018].

[15] Liquid Crystal Technologies, http://www.liquidcrystaltechnologies.com/products/lcdshutters.htm, 2017, [Online; accessed 1-April-2017].

[16] Alluxa, https://www.alluxa.com/, [Online; accessed 1-Jan-2018].

[17] Dejan Nedelkovski, https://howtomechatronics.com/tutorials/arduino/arduino-color-sensing-tutorial-tcs230-tcs3200-color-sensor/, [Online; accessed 1-Jan-2018].

[18] Y.-L. Wei, C.-J. Huang, H.-M. Tsai, and K. C.-J. Lin, "Celli: Indoor positioning using polarized sweeping light beams," in *ACM MobiSys*, 2017, pp. 136–147.

[19] P. Patnaik, *Dean's analytical chemistry handbook*. McGraw-Hill New York, 2004, vol. 1143.

[20] Solid Apollo, https://www.solidapollo.com/LED-UFO-Waterproof-High-Bay-100W-5000K.html, [Online; accessed 14-March-2018].

[21] Amazon, https://www.amazon.com/Polarization-Polarizer-Educational-Physics-Polarized/dp/B06XWXRB75/ref=sr_1_2?ie=UTF8&qid=1523162426&sr=8-2&keywords=linear+polarizing+film, 2017, [Online; accessed 4-Nov-2017].

[22] Thorlabs, https://www.thorlabs.com/newgrouppage9.cfm?objectgroup_id=145, [Online; accessed 1-April-2017].

[23] Amazon, https://www.amazon.com/gp/product/B01CCIKB5Q/ref=oh_aui_detailpage_o04_s00?ie=UTF8&psc=1, [Online; accessed 14-March-2018].

[24] J.-H. Kim, S. Kumar, and S.-D. Lee, "Alignment of liquid crystals on polyimide films exposed to ultraviolet light," *Physical Review E*, vol. 57, no. 5, p. 5644, 1998.

[25] Hamamatsu, https://www.hamamatsu.com/resources/pdf/ssd/s6801_etc_kpin1046e.pdf, 2017, [Online; accessed 1-April-2017].